STAR Note 433
April 11, 2001

Data Analysis Report
To the STAR EMC Collaboration

Comparison of STAR BEMC Responses to Electrons and Penetrating Charged Particles in the Beam-Test-'98

V. L. Rykov* and A. N. Vasiliev¶

Abstract: The responses of the STAR Barrel Electromagnetic Calorimeter (BEMC) to penetrating charged particles and electrons are compared, using data from the BEMC Beam-Test-'98.

1 Introduction

In the STAR BEMC project [1], the measurement of BEMC towers' responses to penetrating charged particle hits[1] from physics events at the running RHIC had been suggested as a base-line method for the BEMC calibration, equalization, and continuous monitoring its stability, particularly early in the program. In details, this technique along with the estimates for its errors, has been described elsewhere [1, 2].

The calibration scheme, using MIP-hits, consists of two stages. At the first stage, a number of BEMC modules is exposed to the external beam, for example at the AGS, and the ratios of towers' responses to MIPs and electrons of various momenta (e/MIP-ratios[2]) are measured. At the second stage, after the modules have been installed in their places in STAR, and RHIC is producing collisions, the samples of MIP-hits from physics events are accumulated, and the position of MIP-peak is measured for each tower. This step essentially completes the procedure of transferring beam-test results to STAR. For the towers exposed to the test beam, their responses to electron hits[3] can immediately be predicted, using measured at the first stage e/MIP-ratios. For non-tested modules[4], these ratios are expected to be close to those of the tested ones, provided the key design tolerances were kept [1, 2, 3].

In this report, we attempt to evaluate e/MIP-ratios in the STAR BEMC, using the experimental data from the BEMC module test at the AGS B2 test-beam in December 1998.

2 STAR BEMC

The STAR Barrel Electromagnetic Calorimeter, a sampling scintillator-lead calorimeter with the pseudo-rapidity coverage of $-1 < \eta < +1$ and 2π in azimuth φ, has been described elsewhere [1, 4, 5]. It will

*Wayne State University, Detroit, Michigan 48202, USA
¶Institute of High Energy Physics, Protvino, 142284, Russia

[1] In this report, we will loosely call this particles as "Minimum Ionizing Particles", MIP, producing "MIP-hits" in the BEMC towers.

[2] The notation "e" is used here for the ratio $S_e(E_e)/E_e$, where $S_e(E_e)$ is the mean BEMC signal from electrons of energy $E_e \equiv P_e c$.

[3] ...of the momenta actually used in the test beam runs ...

[4] ...as well as for all modules at the momenta out of the test beam range ...

be installed within the STAR magnet at the radius of ∼220 cm just outside the Time Projection Chamber (TPC) and Central Trigger Barrel (CTB).

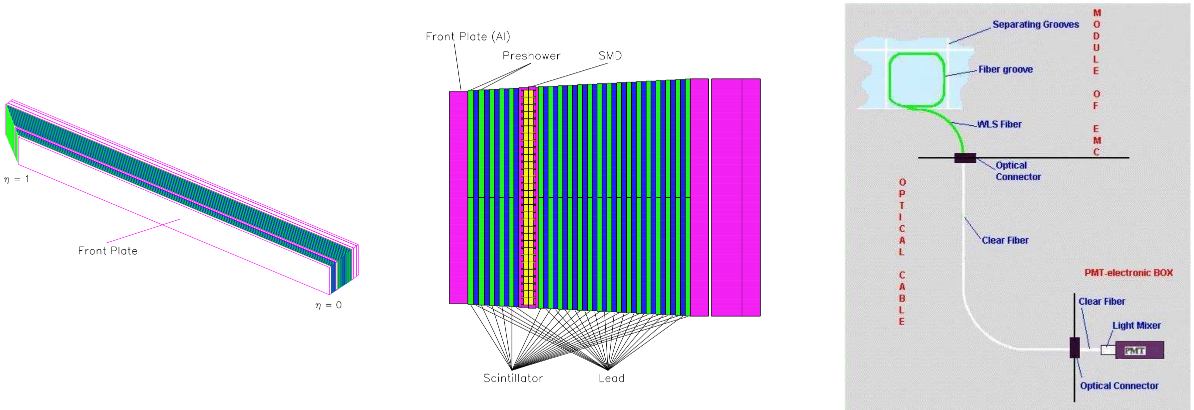

Figure 1: STAR BEMC module view (left), its cross section (center), and light collection scheme(right).

The BEMC consists of 120 modules of the size $\Delta\eta \times \Delta\varphi \simeq 1{\times}0.1$ each. The BEMC module (Fig. 1) is a stack of 21 scintillator megatiles, separated by 5 mm lead sheets. Each megatile is divided into 40 light-insulated tiles, 20 in η by 2 in φ, with a separate readout from each tile, using wave-length shifting fibers connected to ∼3 m long clear fibers. The light from each set of 21 tiles of different layers, which creates a single projective tower of the size $\Delta\eta \times \Delta\varphi \simeq 0.05{\times}0.05$, is collected at a single phototube (PMT), one per tower, totaling in 4,800 channels for the full BEMC coverage. Two front tiles of each tower, with a second set of embedded fibers to transport the light to a separate photodetector, represent a so called "Preshower" (PRS), which is intended to enhance e-γ/hadron separation in the BEMC [6]. To compensate ∼20% loss of light due to a second fiber, two front megatiles were made 6 mm thick, while the thickness of the remaining 19 ones is 5 mm each. For perpendicular tracks, the total BEMC depth is ∼18 radiation lengths (∼$18X_0$) and ∼0.8 of the nuclear absorption length. The position-sensitive two-layer gaseous Shower-Maximum Detector (SMD) is placed in front of the 6th megatile at the depth of approximately $5X_0$ within BEMC stack.

3 Experimental setup at the AGS B2 test beam

For the Beam-Test-'98, the full scale BEMC module with 8 instrumented towers at various η-locations had been built. The extruded polystyrene based scintillator from UNIPLAST (Vladimir city, Russia) has been used for the tiles with the embedded multiclad Kuraray Y11 wave-length shifting (WLS) fibers of the diameter 0.83 mm. The light has been transported to the PMTs, HAMAMATSU-R6427 tubes, using the multiclad Kuraray clear fibers of the diameters 0.9 mm – outside the PMT box – and 1 mm – inside the PMT box. The signals from photodetectors, along with all other signals, have been delivered to the high speed transputer data acquisition system (DAQ) [7]. However, to avoid a saturation of PMT bases, the beam intensity in the expositions has been kept quite low: no more than $\sim(5\text{–}6){\cdot}10^3$ triggers per two-second spill.

The layout of the BEMC test at the AGS B2 beamline is shown in Fig. 2. The module has been positioned at the distance of ∼4.5 m downstream Cherenkov counter C2 and exposed to the negative beam of momenta from ∼0.5 to 7 GeV/c. The event trigger was a coincidence of signals from the beam counters T1/2 and T3. In the data analysis, track positions relative to the BEMC tower were determined, using the two-plane scintillator hodoscope H1/2 with 2 mm spatial bin width. Veto counter V1/2 with the hole of diameter 13 cm has been used to suppress events with the hard scattered in the channel beam particles[5]. Cherenkov counters C1 and C2 were used to tag beam electrons and separate them from pions and other particles. To select "muon" events, three scintillator counters, $\mu1$–$\mu3$, had been installed behind the BEMC module. 25 cm of lead have been placed in between $\mu1$ and $\mu2$, and 55 cm more lead separated $\mu3$ from $\mu2$.

For the most instrumented towers, two sets of measurements had been performed: 1) measurements of the tower responses and 2) evaluation of the light yield from each tile. To measure the tower responses,

[5] Small veto counter + a "finger", V3/F, which is also shown in Fig. 2, has been used only for the SMD study.

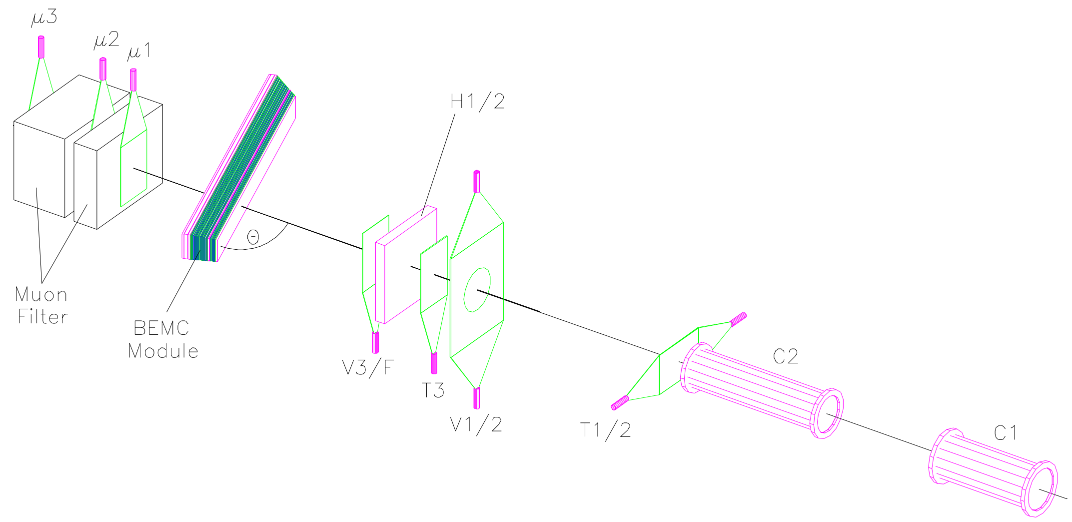

Figure 2: Layout of the BEMC Beam-Test-'98 (not in scale). Rotation angle $\Theta = 90^o - 2 \cdot \arctan(e^{-\eta})$, where η is a projected pseudorapidity position in STAR for the tower under irradiation.

fibers from all 21 tiles in a tower were directed to a single PMT, and one more PMT was used to measure the combined signal from two PRS tiles. To measure and compare light yields from the tiles, an individual PMT has been used for each of 21+2 fibers in a tower. In these "tile-to-tile" measurements, each PMT signal has been additionally amplified by a factor of ~100 times, using the chain of two LeCroy 612A amplifiers.

4 Tower responses to electrons and MIPs

For each run, three main signal distributions in a tower, # 40, 42 and 43, have been analyzed (Fig. 3). Hits in histograms #40 and #43 were subsets of those in #42 (all triggers), selected around the center of an exposed tower and restricted to the area of $\sim 3 \times 3$ cm^2 in the hodoscope H1/2. Cuts from veto counter V1/2 had also been applied. Then, events have been sorted out to electrons and MIPs (not electrons), using Cherenkov counters C1 and C2.

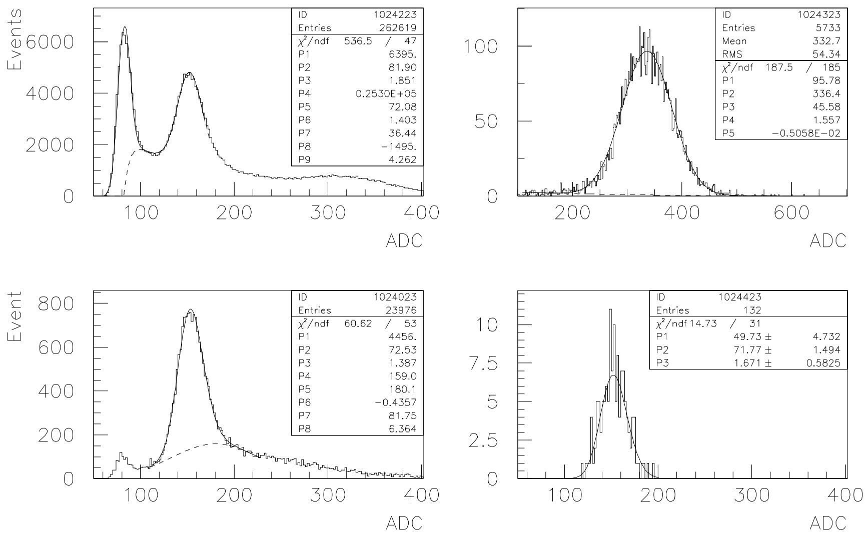

Figure 3: Signal distributions for the tower R2T2 ($0.05 < \eta < 0.1$) at P_{beam} = 1 GeV/c: #42 ≡ "rrr42cc" (upper-left frame) is for all triggers; #43 (upper-right) is for electrons; #40 (lower-left) is for MIPs (not electrons), centered at the tower, using the hodoscope, and sorted out with Cherenkov counters; #44 (lower-right) is a subset of #40, selected in coincidences with $\mu 1$ & $\mu 2$ counters. In the histogram IDs above, "rrr" is for the run number and "cc" is for the DAQ channel number. Fits to background are shown with the dashed lines (for histogram #42, the shown "background" is actually the full fit (2), less the pedestal gaussian).

For the known[6] pedestal's peak position (PED) and width (σ_{PED}), MIP peak positions have been determined from 6-parameters fits to histograms #40. It was found that Vavilov distributions [8] quite satisfactorily approximate the energy deposits simulated with GEANT from penetrating charged particles[7] in the BEMC towers. To account also for the photon and secondary-electron statistics in the PMTs, electronics noise, and background from hadron interactions and decays under and in the vicinity of MIP peaks, the following function had been used to fit histograms #40:

$$F_{MIP}(x) = a \cdot \int_{PED}^{\infty} \frac{dy\, \exp\left(-\frac{(x-y)^2}{2\sigma^2(y)}\right)}{2\pi\sigma(y)} \Phi_V\left(\frac{y - PED - MIP}{s \cdot MIP} + \overline{X}_{\Phi}(\kappa,\beta^2)\,;\,\kappa,\beta^2\right) + b_0 \cdot \exp\left(b_1 x + b_2 x^2\right) \quad (1)$$

where:

$\Phi_V(\lambda;\kappa,\beta^2)$ is Vavilov distribution VAVDEN from CERN library [9];

$$\sigma(y) = \sqrt{\sigma^2_{PED} + \alpha \cdot (y - PED)}$$ is the width of the smearing gaussian;

$$\overline{X}_{\Phi}(\kappa,\beta^2) = \frac{\int_{-\infty}^{\infty} \lambda \Phi_V(\lambda;\kappa,\beta^2)\, d\lambda}{\int_{-\infty}^{\infty} \Phi_V(\lambda;\kappa,\beta^2)\, d\lambda}$$ is the mean value of the "bare" Vavilov distribution $\Phi_V(\lambda;\kappa,\beta^2)$;

MIP is what is called here "MIP peak position", that is the mean over MIP peak with already subtracted PED and corrected to the background;

b_0, b_1 and b_2 are parameters of the smooth function to fit background.

Constants κ, β^2 and s were selected individually for each tower's η-position and beam momentum from the best Φ_V-fits to the simulated MIP energy deposits in the BEMC. From 6 parameters: a, MIP, α, b_0, b_1 and b_2, which were to be determined from the fits, only one was actually the goal[8], that was MIP. Fits to histograms #40 were usually extended from $PED + 4 \cdot \sigma_{PED}$ to $PED + 2 \cdot MIP$. According to simulations, systematic errors[9] of MIP reconstruction, using fit (1), should be expected at about $\pm 0.7\%$ for the photoelectron yields $N_{phe}(MIP)$ at or above $\sim$40 phe/tower.

Histograms #44, obtained in coincidences with muon counters $\mu 1$ & $\mu 2$, represent MIP peaks in the towers virtually without background from hadron interactions and decays. 3-parameter fits (1) to histograms #44 with $b_0 = 0$[10] always produced MIP values consistent with those obtained from the respective distributions #40. However in most cases, due to reduced numbers of events, particularly at low beam momenta, the statistical errors for MIP-parameter from distributions #44 were much larger compared to the ones from histograms #40.

The pedestals and their widths have been determined from the fits to the histograms #42 with the function similar to that of Eq. (1):

$$\begin{aligned} F_{PED}(x) &= c \cdot \exp\left(-\frac{(x-PED)^2}{2\sigma^2_{PED}}\right) + \int_{PED}^{\infty} \frac{dy\, \exp\left(-\frac{(x-y)^2}{2\sigma^2(y)}\right)}{2\pi\sigma(y)} \times \\ &\times \left[a \cdot \Phi_V\left(\frac{y - PED - MIP}{s \cdot MIP} + \overline{X}_{\Phi}(\kappa,\beta^2)\,;\,\kappa,\beta^2\right) + b_0 \cdot \exp\left(b_1(x-y) + b_2(x-y)^2\right)\right] \quad (2) \end{aligned}$$

The differences are that, in Eq. (2), a gaussian fit to pedestal peaks is added, and the background function is also convoluted with the smearing gaussian the same way as Φ_V. Three more free parameters: c, PED and σ_{PED} were added, bringing the total number of parameters in fit (2) to 9. Out of them, only two, PED

[6] i.e., extracted from histograms #42; see below.

[7] The composition of B2 negative beam was mainly π-mesons with some fraction of kaons, electrons, and muons. In the simulations, negative pions have been taken for MIPs.

[8] Actually, parameter α also carries useful information about the light yield from a tower. In terms of Ref. [10] (see also [11]), $\alpha = G \cdot MIP/N_{phe}(MIP)$, where $N_{phe}(MIP)$ is the mean number of photoelectrons from MIPs, crossing a tower; G is the factor derivative from the secondary-electron statistics in a PMT. The simulations have shown that the errors of $N_{phe}(MIP)$ estimates, using α from fits (1), were at about $\pm$(15–20)%.

[9] Not accounting statistics and error of PED knowledge.

[10] ...as well as just simple means over these histograms ...

and σ_{PED}, were utilized in further analysis[11]. At high statistics of up to 10^6 events, the quality of fits to histograms #42 had never been exceptionally good. However, parameters of interest, PED and σ_{PED}, were sensitive to only the height and slope of the signal distribution just immediately to the right of the pedestal peak and not sensitive to the fit quality in remote areas. From the study of simulated similar distributions, it was found that fit (2) systematically shifts PED to the right, in average, bye $\sim 0.03 \cdot \sigma_{PED}$. The deviations (RMS)[12] of the reconstructed PEDs from true values fluctuated from case to case at $\sim(0.1\text{–}0.12) \cdot \sigma_{PED}$. With σ_{PED} varied from 2 to 6.5 ADC, this gives the estimate for the PED reconstruction errors in the range from $\sim \pm 0.2$ to ± 0.7 ADC counts.

Mean positions and widths of electron signal distributions were determined from a simple 3 parameter gaussian fit to histograms #43. Sometimes, 4 or 5 parameter fits had been used to account for a background under an electron peak, which has been approximated with a constant or exponential.

In Fig. 4, the "raw" data for the BEMC towers' responses to electron hits are shown. Each instrumented tower has been exposed to the beam in several[13] exposition runs at nominal B2 momentum settings of $P_{beam} = 0.5$, 1, 2, 5 and 7 GeV/c. As it has been pointed out in Ref. [12], the actual particle momenta, when they approach the BEMC module location, are lower than the nominal settings due to energy losses in the beamline. The simulations with GEANT suggested electron momentum corrections at about 25–30 MeV/c which are quite close to the measurements [12]. The positioning of the experimental points in the plots of Fig. 4 and elsewhere in this section reflects these corrections.

The ratios $e(P)/\text{MIP}(P = 1 \text{ GeV/c})$ in the bottom row, which were actually the goal of this analysis, have been obtained in the following ways. For the towers R1T11 at $\eta \simeq 0.5$ and R2T19 at $\eta \simeq 1$, the simple and straightforward approach has been used. Namely, $e(P)$ values from the upper row of Fig. 4 have been divided by $\text{MIP}(P = 1 \text{ GeV/c})$ for the same tower, averaged over all runs at $P_{beam} = 1$ GeV/c. For the tower R1T10 with the only exposition at $P_{beam} = 5$ GeV/c, this ratio had been evaluated from the measured $e(5 \text{ GeV/c})/\text{MIP}(5 \text{ GeV/c})|_{R1T10}$, which then has been transformed to $e(5 \text{ GeV/c})/\text{MIP}(1 \text{ GeV/c})|_{R1T10}$, using $\text{MIP}(5 \text{ GeV/c})/\text{MIP}(1 \text{ GeV/c})|_{R1T11}$ ratio, measured for the tower R1T11.

The approach above is obviously applicable to the towers at $\eta \simeq 0$ too. However, since more than one tower at $\eta \simeq 0$ had been exposed to the beam, this provided the opportunity to try also a slightly different way for obtaining $e(P)/\text{MIP}(1 \text{ GeV/c})$-ratios[14]. It was reasonable to assume that, for the towers at approximately same η, there must be one universal $\text{MIP}(P)$ dependence, which could be reconstructed from the data and then used to transfer $e(P)/\text{MIP}(P)$ to $e(P)/\text{MIP}(1 \text{ GeV/c})$ for all 4 towers. This "universal" $\text{MIP}(P)$ dependence for $\eta \simeq 0$ is shown in Fig. 5 along with the experimental points, normalized to MIP(1 GeV/c). It is based on the restricted energy loss function from Ref. [13] with the medium characteristics from Ref. [14]. This function quite satisfactorily describes the GEANT simulated $\text{MIP}(P)$ dependence at $\eta = 0$ for pions in the momentum range 0.5–7 GeV/c with parameter $T_{cut} = 0.43 \cdot 10^{-3} \times \text{Pc}$. $\text{MIP}(P)$ dependence in Fig. 5 is actually a 3-parameter fit (T_{cut} and two normalization constants)[15] to the combined data from towers R1T2a and R2T1. These two towers have been chosen because they had been exposed to 2 GeV/c beams before and after exposing them at other momenta. The comparison of different expositions at $P_{beam} = 2$ GeV/c did not reveal any changes of signals beyond the measurement errors. This allowed us to assume that there had been no substantial drifts of the PMT/ADC gains during the entire measurements at these two towers, which could potentially interfere with $\text{MIP}(P)$ dependence.

From the data of Fig. 4 it follows that, in the Beam-Test-'98, the towers' responses to electron hits were not exactly proportional to electron energies. The nonlinearities were quite large, up to $\sim$10–15%. Meanwhile, on the basis of multiple simulations with GEANT, the STAR BEMC by design is expected to be linear within $\sim \pm(0.2\text{–}0.5)$%. The other striking observation is that e/MIP-ratios for different towers at $\eta \simeq 0$ are different by up to $\sim$30%. In the rest of this section, we will attempt to understand such a behavior of "raw" data, attributing it to variations of light yields from tile to tile in each tower, and also to the electron shower leaks from the towers of finite transverse dimensions. The corrected data will then be used to evaluate the expected mean e/MIP-ratios for the BEMC modules in STAR, which will presumably

[11] Quite often, parameter MIP from fit (2) was close to the one from fit (1). However, it had never been trusted because of MIP peak shape distortion in the distributions #42 by peripheral hits, etc., which was particularly noticeable at low beam momenta.

[12] ... beyond pure statistics ...

[13] From one (R1T10) to eight (R1T2a & R1T11).

[14] Actually, both approaches gave similar results.

[15] This fit yielded parameter $T_{cut} = (0.65 \pm 0.25) \cdot 10^{-3} \times \text{Pc}$.

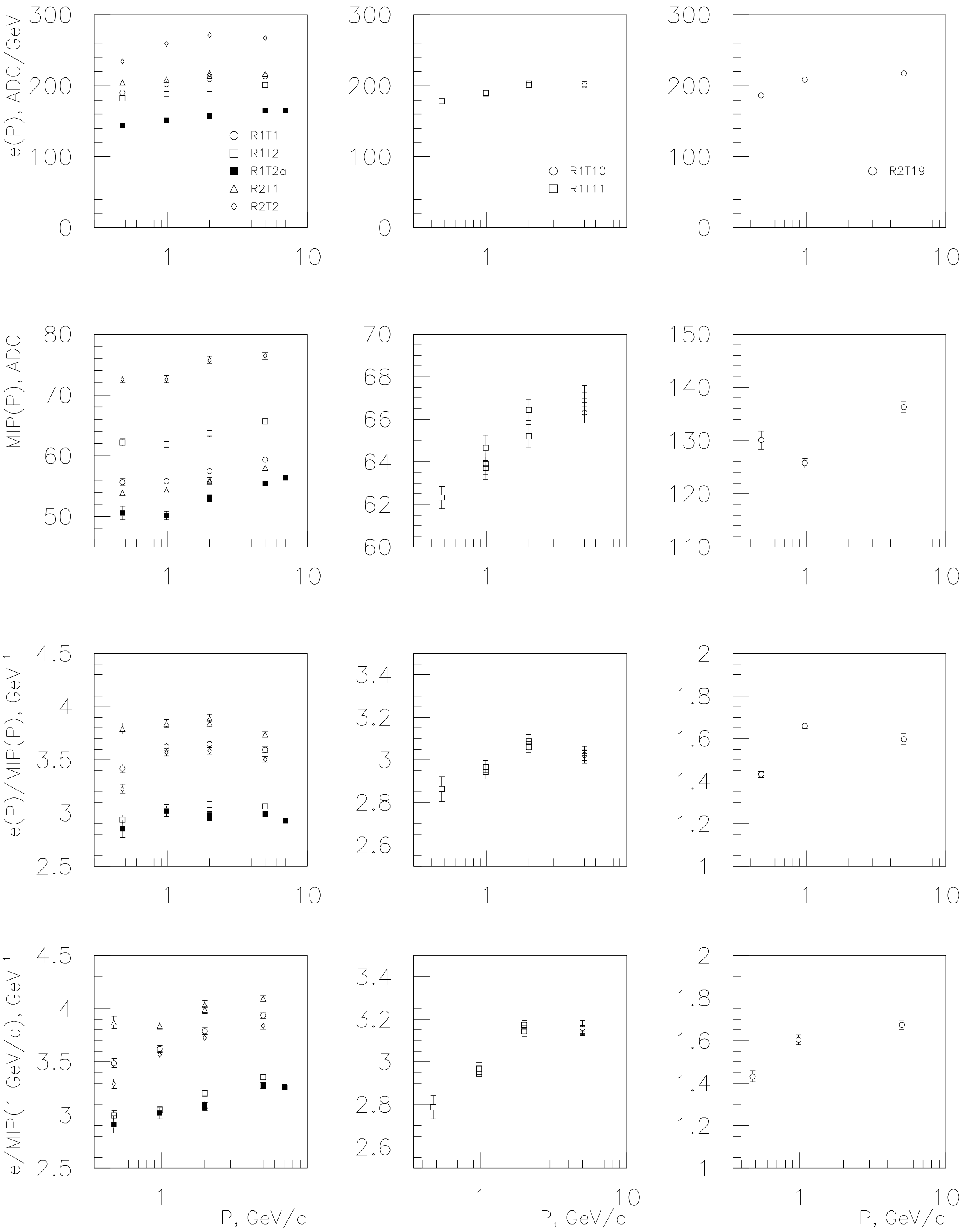

Figure 4: Raw data for the towers' responses to electrons and MIPs. Left, middle and right columns are for the towers at $\eta \simeq 0$, 0.5 and 1, respectively. The convention for the tower's enumeration is as following: tower "RnTm" was located at $0.05\cdot(\text{m-1}) < \eta < 0.05\cdot\text{m}$ in the lower (n=1) or upper (n=2) module's row. The notation R1T2a is for the measurements at the tower R1T2 with the lowered PMT gain and subsequent $\sim$10-fold PMT signal amplification, using LeCroy 612A amplifier. Error bars include only statistics and systematic errors of fits which have been discussed in pages 4 and 5.

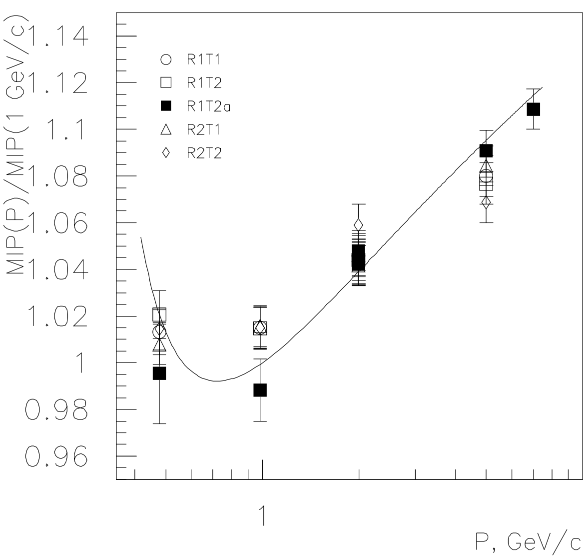

Figure 5: MIP(P) dependences for $\eta \simeq 0$, normalized to MIP(1 GeV/c).

be built in compliance with the design specifications.

In Fig. 6, left frame, the GEANT simulated towers' responses to electrons of various momenta are compared. Electron shower leaks from a tower to its neighbors, simulated for a close to the actual test-beam layout and event selection, and the measured variations of light yields from tile to tile[16] have been accounted. The results are normalized to "ideal" towers, which were the towers with an uniform light yield from all tiles[17], equal to the mean yield from the respective "real"[18] tower. Ideal towers have been taken wide enough to neglect shower leaks out to their neighbors[19]. One can observe that the simulated differences of "real"

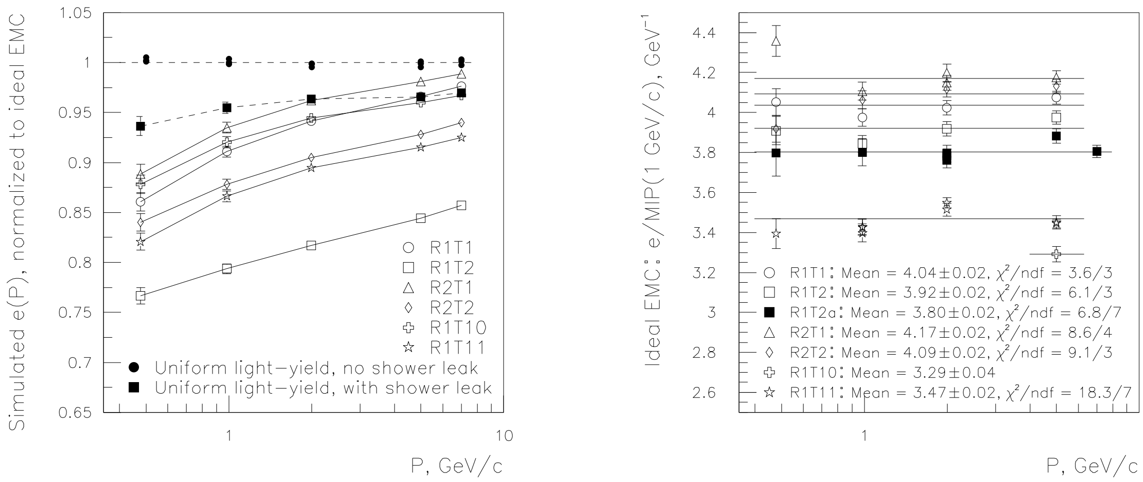

Figure 6: e/MIP(1 GeV/c)-ratios (right frame), corrected to the non-uniformity of light yields from the tiles and shower leaks from the towers, using simulations shown in the left frame. Tower R2T19 is not present in this figure because of no data from tile-to-tile measurements were available for this tower to evaluate correction.

towers' responses and of the "ideal" ones are really quite large, up to ∼25%. The contribution of the shower leaks only was at ∼5%. Slightly larger leaks at low momenta were due to larger effect of electron multiple scattering in the air downstream the hodoscope, resulting in a noticeably larger irradiated area at a tower

[16] See Sec. 5.

[17] For the first two tiles, the light yields have been assumed at 80%, compared to all other tiles, per equal ionization energy deposits.

[18] i.e., used in the beam-test.

[19] In STAR, actually the sums of signals from adjacent towers will be used for S_e to determine an electron energy.

compared to the fiducial spot size for the selected tracks in the hodoscope plane.

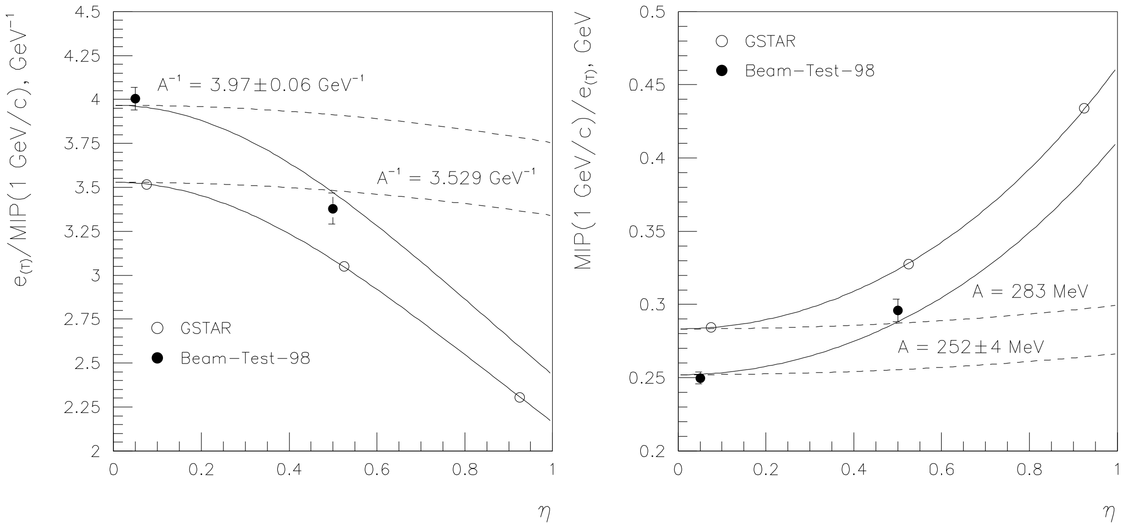

Figure 7: Comparison of measured and simulated e/MIP-ratios (left frame) and of their inversed, the Equivalent Electromagnetic MIP Signals, $EEMS$ = MIP(1 GeV/c)/e (right frame). Solid lines are for e/MIP- and dashed lines are for e_T/MIP-ratios (and respective inversed), where $e_T = S_e(E_e)/E_T$ and $E_T = E_e \sin\theta$ (see footnote 2 in Sec. 1 for other notations).

By dividing the measured e/MIP(1 GeV/c) for each tower (Fig. 4, bottom row) by the respective combined corrections from Fig. 6 (left frame), we should presumably predict e/MIP-ratios for the "ideal" BEMC towers. The results of this operation are shown in the right frame of Fig. 6. It is apparent that, for all towers, e/MIP(1 GeV/c) momentum dependences became more "flat" compared to the "raw" data. Actually, all these dependences are consistent with constants within $\sim \pm$(1–1.7)$\cdot\sigma$, in average, where σ is for the error bar estimates from the known sources discussed above. However, even for the towers of the same η, the momenta averaged e/MIP-ratios differ from each other by $\sim \pm 3.7\%$ (RMS), which is well beyond their statistical errors of $\pm$(0.5–1)%. This means that, probably, there were some other factors which affected the measured data but have not been accounted in the simulated corrections. Among them could be, for example, slightly different towers' alignments at the beam, which made shower leak effects individual for each tower. The other loophole is that the measured ligh-yield variations from tile-to-tile, which then have been used in the simulations, do not exactly correspond to the ligh-yield variations in the measurements of towers' responses. Unaccounted differences in the light transmission for two different setups from the last optical connector down to the PMTs and also unaccounted variations of PMT's quantum efficiencies in the tile-to-tile measurements, to our estimates, could lead alone to the correction uncertainties at about $\pm 3\%$. Another $\sim \pm$(3-5)% might arrive from ADC nonlinearities which, according to the specification [15], could be as large as ± 0.5 pC, i.e. ± 2 ADC channels. It is worth mentioning that the ADC nonlinearities, if they were similar in different channels, could also make a systematic shift to all measured e/MIP-ratios.

The final estimates for e/MIP-ratios for two η-positions could be obtained by taking simple averages over the corrected means from Fig. 6 for the towers at $\eta \simeq 0$ and 0.5. This gives the following results:

$$e/\mathrm{MIP(1\ GeV/c)}|_{\eta=0.05} = 4.00\times(1\pm0.016_{stat}) \quad (3)$$
$$e/\mathrm{MIP(1\ GeV/c)}|_{\eta=0.50} = 3.38\times(1\pm0.021_{stat}) \quad (4)$$

In Fig. 7, these numbers are compared to the simulations with GSTAR[20] for the "ideal" BEMC. Functionally, the experimental η-dependence of e/MIP-ratio is in agreement with the fit to the simulated points:

$$e/\mathrm{MIP(1\ GeV/c)} = A^{-1} \times (1 - 0.054 \cdot \eta^2) \times \sin\theta\ , \quad (5)$$

[20]GSTAR is the configured with STAR setup version of GEANT.

where $\theta = 2 \times \arctan(e^{-\eta})$. However, the normalization constants A differ from each other by ∼12%. This difference might partially be due to experimental uncertainties, which have been discussed in the previous paragraph. The underestimation by GSTAR of e/MIP-ratios at ∼(5–10)% cannot be excluded either. Keeping all these in mind, it would probably be fair to estimate the scale error of the final results in Fig. 7 at about ±(4–5)%.

5 Light yields from the scintillator tiles

The measurements of light yields from the tiles[21] pursued two goals. The first goal was to evaluate the absolute yield of photoelectrons from a certain energy deposit in a tile. Earlier, it has been determined that, to meet the design specifications for the BEMC energy resolution and dynamic range, the mean photoelectron yield must not be less than 2 phe/tile for perpendicular MIP crossings [1]. The other goal was to measure the variations of light yields from tile to tile which, according to the specification [1], must not exceed 10% (RMS) for keeping the BEMC linear within required ±2%.

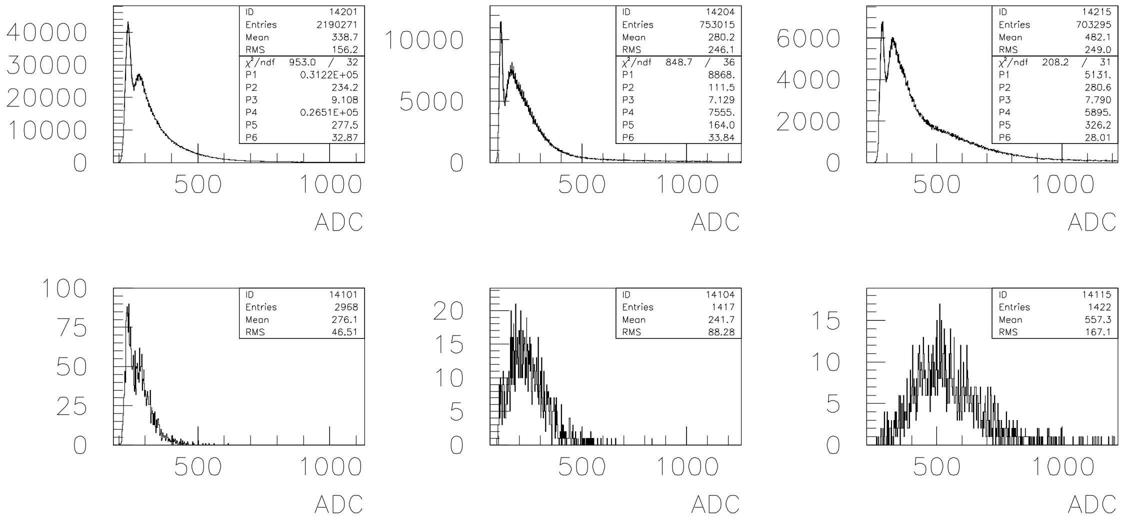

Figure 8: Typical signal distributions from the tiles. "All triggers" histograms are shown in the upper row. The lower row represents MIP-hits. MIPs have been selected as not electrons in C1–C2, centered with the hodoscope, and in coincidences with $\mu 1$ & $\mu 2$ counters.

All tile-to-tile measurements had been carried out at $P_{beam} = 2$ GeV/c. For each tile, two types of histograms have been analyzed (Fig. 8). Each channel's pedestal and gain in ADC-counts/phe were determined from "all-triggers" histogram. For this purpose, a simultaneous fit of two overlapping gaussians has been applied to the interval, which contained a pedestal peak and a "single photoelectron" peak (SPP) to the right of the pedestal. Actually, these SPP peaks were not true single-phe ones but included also large contributions of signals from 2, 3 and more photoelectrons. Therefore, it was not obvious, which particular procedure should be used to correctly evaluate the SPP position from "all triggers" histograms with acceptable systematic errors. The special simulation study has shown that two-gaussian fits, applied over the limited intervals around two peaks, could be used to determine true SPP positions at the accuracy[22] of about ±3-5%. This procedure had also been cross-checked, using the experimental data, with the light-emitting diode technique from Refs. [10, 11] for measuring absolute PMT gains. The results of two approaches were consistent within errors.

The tile-to-tile measurements have been analyzed for four towers at $\eta \simeq 0$, two towers at $\eta \simeq 0.5$, and one tower at $\eta \simeq 1$. No noticeable differences of the channel gains have been detected in the measurements at different towers of the same η, because all measurements at fixed η had usually been carried out within

[21] Which are also referred here as "tile-to-tile" measurements.
[22] Not accounting the statistics.

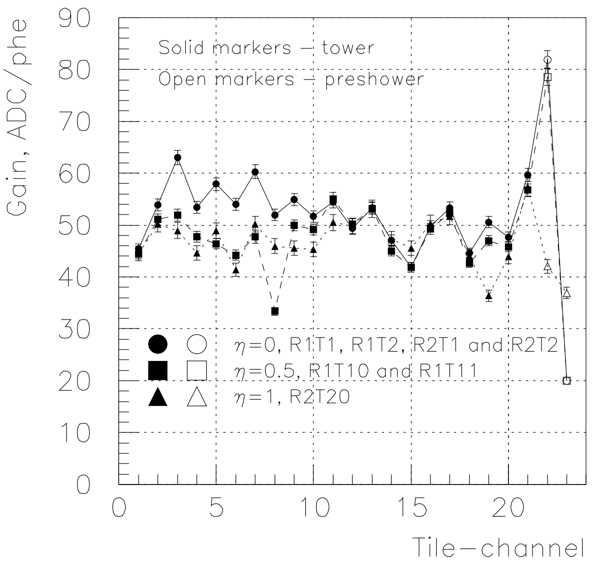

Figure 9: Channel gains in the tile-to-tile measurements.

a quite short time interval. Therefore, just 3 sets of averaged gains have been used in further analysis, i.e. one "universal" set has been applied to all towers of the same η-position. These 3 sets of measured gains are shown in Fig. 9.

The absolute light-yield from each tile has been calculated by dividing the mean value over respective MIP-histogram (bottom row of Fig. 8), less pedestal, by the channel's gain from Fig. 9. The results are shown in Fig. 10. Apparently, for all seven analyzed towers, mean yields for perpendicular MIP crossings were well above the required 2 phe/MIP, although the yield variations from tile to tile within a tower fell short from satisfying the design specification of no more than $\pm 10\%$ (RMS). The noticeably lower than average yields from 1st, 2nd and 11th tiles in most towers[23] point out to the presence of some common causes for such a behavior. This is not a surprise, however, because the same bundles of clear fibers downstream the first optical connector and, obviously, PMTs had been used in the measurements at different towers. It should be underlined that the light yield variations in these measurements also include the contribution of variations of photocathode quantum efficiencies from channel to channel. This contribution had not been present in the measurements of towers' signals, because in this case all fibers from a tower were directed to a single PMT.

Conclusion

On the basis of this analysis, it is suggested that, for a time being before the more comprehensive BEMC beam test data are available, the following expression for the Equivalent Electromagnetic MIP Signal (EEMS) could be used for the purpose of STAR BEMC calibrations at the running RHIC:

$$EEMS \equiv \mathrm{MIP}(1\ \mathrm{GeV/c})/e = \frac{A}{(1 - 0.054 \cdot \eta^2) \times \sin\theta}$$

with $A = 252 \times (1 \pm 0.015_{stat} \pm 0.05_{sys})$ MeV.

The analysis of Sec. 5 has shown that, for all instrumented towers in the Beam-Test-'98, the mean photoelectron yields from the tiles were above the minimum required 2 phe/MIP with good safety margins. However, the measured light yield variations within any single tower were larger than $\pm 10\%$ allowed by the design specification.

[23] ...and also from the preshowers ...

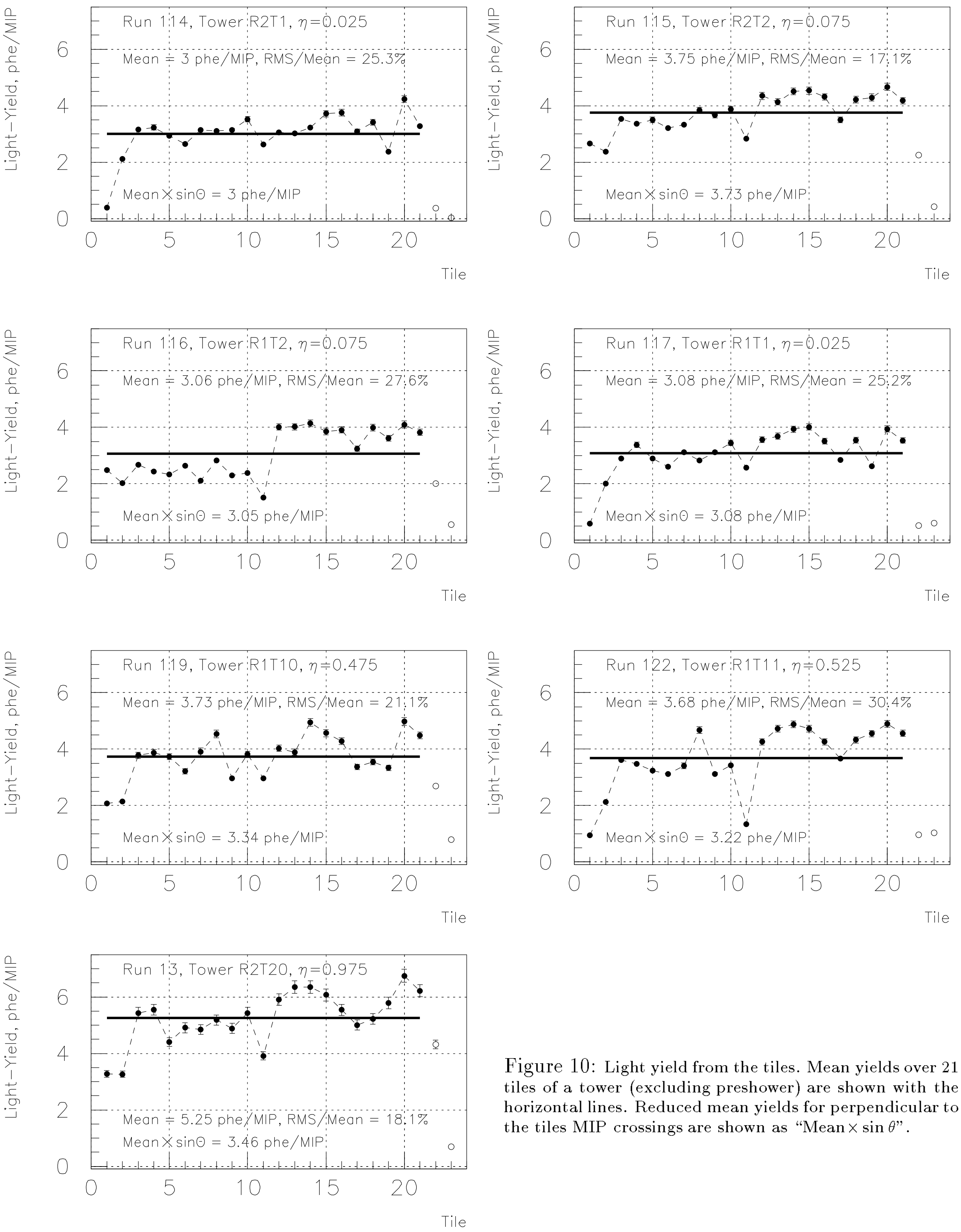

Figure 10: Light yield from the tiles. Mean yields over 21 tiles of a tower (excluding preshower) are shown with the horizontal lines. Reduced mean yields for perpendicular to the tiles MIP crossings are shown as "Mean $\times$ sin θ".

Acknowledgments

It is our pleasure to present this long overdue data analysis report to the STAR EMC Collaboration members who built the prototype and carried out these beam measurement.

References

[1] STAR EMC Collaboration, STAR EMC Technical Design Report, 1998.

[2] S. Bennett, et al., Annual report of the WSU Nuclear Science Group to the DoE, 1999, p. 133; T. M. Cormier, et al., STAR Note in preparation, 2001.

[3] A. A. Derevschikov, O. D. Tsai. STAR Note 216, 1995.

[4] J. W. Harris, et al. (STAR Collaboration at RHIC), Nucl. Phys. **A566** (1994) c277–c286; STAR Collaboration, Conceptual Design Report for the Solenoidal Tracker At RHIC, BNL PUB-5347, June 15, 1992.

[5] W. J. Llope (for the STAR-EMC Collaboration), Proc. VI International Conference on Calorimetry in High Energy Physics, 1996, Frascati Physics Series, v. VI, p. 187.

[6] S. Chattopadhyay, et al., STAR Note 414, 1999; T. J. LeCompte, STAR Note 306, 1997.

[7] A. Vander Molen, et al., IEEE Trans. on Nucl. Sci., **NS-41**, No 1 (1994) 80.

[8] P. V. Vavilov, Soviet J. Exp. Theor. Phys. **5** (1957) 749.

[9] A. Rotondi, P. Montagna, K. S. Kölbig, CERN Program Library – Short Writeups, http://wwwinfo.cern.ch/asdoc/shortwrupsdir/g115/top.html.

[10] V. L. Rykov, STAR Note 301, 1997.

[11] B. Bencheikh, et al., Nucl. Instr. & Meth., **A315** (1992) 349.

[12] A. Patwa, et al., PHENIX Technical Note 181, 1995.

[13] D. E. Groom and S. R. Klein (Particle Data Group), Eur. Phys. J., **C15** (2000) 165.

[14] R. M. Sternheimer, M. J. Berger and S. M. Seltzer, Atomic Data and Nuclear Data Tables, **30** (1984) 261.

[15] 4300B 16 Input Fast Encoding and Readout ADC, www.lecroy.com/lrs/dsheets/4300b.htm.